Dynamic Modeling and Simulation of an Hybrid Renewable Energy System in Colombia

BENAVIDES, A. E. [a,c*], VALENCIA, G. E. [a,b], CARDENAS, Y. D.[c]

a. Universidad del Atlántico, Barranquilla

b. Universidad del Atlántico, Barranquilla

c. Universidad de la Costa, Barranquilla

**Aldair Enrique Benavides Gamero, aebenavides@mail.uniatlantico.edu.co*

Abstract

The hybrid system switched to the production of electric energy allows supplying the energy demand in Non-Interconnected Zones, contributing both to the improvement in the reduction of greenhouse gas emissions and to the rational use of energy. A comparative analysis of the performance of these systems was supported out in this study for four sites in the Colombian Caribbean region, using a dynamic model programmed in Matlab, which integrated the equations of a Southwest Wind Power Inc. wind turbine. AIR 403, a proton exchange fuel cell (PEM), an electrolyzer, a solar panel and a charge regulator based on PID controllers to manipulate oxygen and hydrogen flows in the cell. The transient responses of the cell voltage, current, and power have obtained for the demand of 200 W for changes in solar radiation and wind speed for all days of the year 2013 in the Ernesto Cortissoz airport, Puerto Bolívar, Alfonso López airport and Simón Bolívar airport, by regulating the flow of hydrogen and oxygen into the fuel cell. The maximum contribution of power generation from the fuel cell was presented for the Simón Bolívar airport in November with a value of 158,358W (9.45%). While the minimum has shown in Puerto Bolívar with 18,141W (3.745%), which allowed to evaluate the changes in the complementarity of these energies for this system. Finally, the simulations of the hybrid energy system allowed us to select Puerto Bolivar's location as the most efficient for the hybrid system's operation because the high potential of wind and solar energy makes it possible to have low consumption of hydrogen and oxygen flow.

Keywords: *Fuel cell, PID control, Hybrid energy system, Caribbean region, simulation.*

1. Introduction

In response to the global problem of greenhouse gas emissions and global warming, many countries have begun to diversify their energy matrix by incorporating renewable energy generation systems [1]–[4]. The potential growth of these generation systems has allowed this solution has positioned as a mature technology in the energy sector [5]–[7], significantly impacting on the improvement of energy and environmental indicators in some nations [8].

In Colombia, national regulations have motivated the rational use of energy and preservation of the environment [9], emphasizing renewable resource generation systems such as solar and wind energy [10]–[12]. However, currently the percentage contribution of these systems is low compared to conventional generation systems, the primary source being hydroelectric with 69.5%, followed by thermal with 29.6% and renewable with a percentage less than 1% (0.9%) [13], which corresponds to the few investigations developed to evaluate the energy performance of hybrid power generation systems, when they operate with the energy resources available in the different regions of the country [14], [15]. Since hybrid power generation systems allow switching the energy source to meet demand, these have been extensively studied when proposing energy solutions in areas not interconnected to the grid [13] [16]–[18].Simulations of this type of the system developed on both small and large scale. [19], in addition to experimental studies [20], even taking into account the tidal energy source with highly sophisticated and robust mathematical formulations [21]. On the other hand, in countries such as Brazil, photovoltaic solar technology has been integrated into hybrid systems [22], since it is a highly reliable and functional energy alternative [23], with advantages such as the use of few parts, low maintenance requirements and quiet operation [24], [25], Even in Mexico, the study of this system in the Veracruz region was being highlighted [26].

The main contribution of this study is to evaluate the complementarity of wind, solar and electric power generation in a proton-exchange fuel cell (PEM), through a dynamic model of a hybrid system operating in different places in the Colombian Caribbean Region for the demand of 200W.

2. Methodology

2.1. Description of the region and information

The Colombian Caribbean region, as shown in Fig. 1, is located in the north of the country with a population of approximately 11 million people, located in the area of roughly 132,270.5 km^2 (11.6% of the national territory). [27]. It is bounded to the north by the Atlantic Ocean, to the east by Venezuela, to the west by the Pacific Ocean and the south by the Andean region, is made up from flat areas except Magdalena and the snow-capped mountains (5).755 m) and a full coastal region. Also with a climatic diversity ranging from tropical to subtropical, where the average temperature is 30°C and even reaching up to 35°C in the Riohacha because of its arid and desert zone. For the evaluation of the hybrid system, data being taken from Ernesto Cortissoz airport, Puerto Bolívar, Alfonso López airport and Simón Bolívar airport meteorological stations, managed by the Instituto de Hidrología, Meteorología y Estudios Ambientales (IDEAM), with time series for temperatures, humidity and wind speed at a height of 10 meters by 2013.

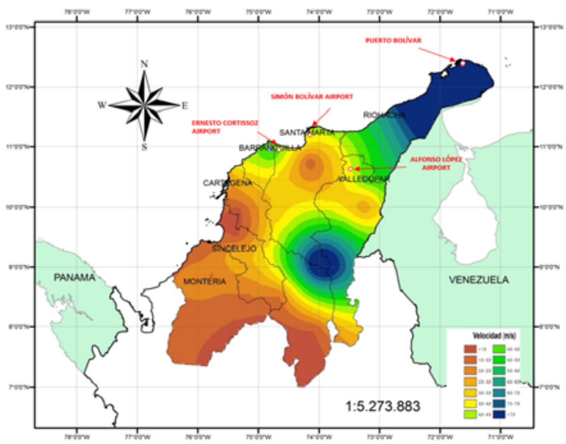

Fig. 1. Geographical location of the places studied in the Caribbean region (Colombia).

3. System description

The hybrid energy power generation system (HEPGS) as shown in Fig. 2 is integrated by a solar power generation module, with a unit power ratio of 37.08 W, a maximum voltage and current of 16.56 V and

2.25 A respectively, for a total of 36 cells in series and 1 in parallel. [28], in addition to a Southwest Wind Power Inc. wind turbine. AIR 403 with the ability to generate a peak power of 820 W at a wind speed of 40 miles/hour. [28], and a PEM fuel cell, which produces 401.23 Watts, a voltage and current of 48 V and 8.26 A, when a molar flow of hydrogen and the oxygen of 0.005 mol/s at 25°C supplied to the chemical reaction. The system was complemented with an electrolyzer for the generation of hydrogen and power regulator that operates with two PID controllers tuned to the Ziegler Nichols method to manipulate the flow of oxygen and the hydrogen that has been supplied to the cell. [29].

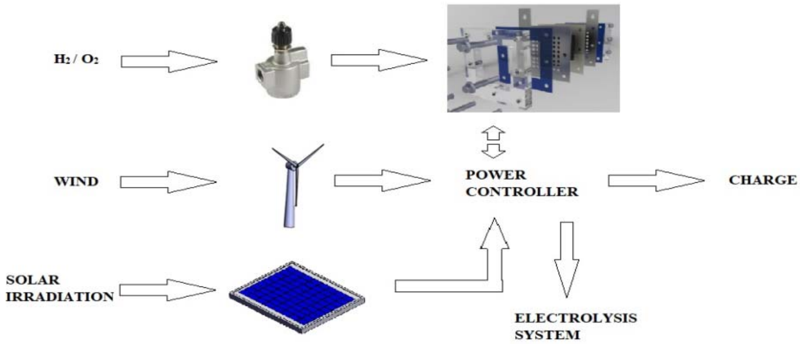

Fig. 2. *Hybrid power generation systems schematic diagram.*

3.2. Dynamic fuel cell model

The dynamics of the PEM type fuel cell has been extensively studied. [30], where the thermodynamic potential E is calculated using the Nernst equation [31], resulting in the equation (1).

$$E = 1.229 - 0.85 \times 10^{-3}(T - 298.1) + 4.3085 \times 10^{-5}\left(lnp_{h_2} + 0.5lnp_{o_2}\right) \tag{1}$$

where T is the fuel cell temperature in Kelvin and the concentration of dissolved oxygen in the gas/liquid interface is defined by Henry's law, as shown in equation (2).

$$Co_2 = \frac{p_{o_2}}{5.8 \times 10^{-6} exp\left(\frac{-498}{T}\right)} \tag{2}$$

Excess stress due to activation and internal resistance is calculated by equations (3) and (4), which are experimental relationships.

$$n_{act} = 0.00312T - 0.86514 - 0.000187\ln(i) + 7.4 \times 10^{-5}TlnCo_2 \tag{3}$$

$$R_{int} = 0.01605 - 3.5 \times 10^{-5}T + 8 \times 10^{-5}i \tag{4}$$

Fuel cell current and activation resistance are related as shown in equation (5).

$$R_a = -\frac{n_{act}}{i} \tag{5}$$

The output voltage of the fuel cell is given by equation (6).

$$V = E + \eta_{ohmic} - V_{act} \tag{6}$$

The dynamics of the activation voltage of the fuel cell is described by equation (7).

$$\frac{dV_{act}}{dt} = \frac{i}{c} - \frac{cV_{act}}{R_a} \tag{7}$$

The loss of the ohmic voltage and the total voltage contained in the fuel cell is described by equations (8) and (9) respectively.

$$\eta_{ohmic} = -iR_{int} \tag{8}$$

$$V_{stack} = 65V_{cell} \tag{9}$$

Anode and cathode pressure are calculated as shown in equations (10) and (11).

$$\frac{V_a}{RT}\frac{dp_{H_2}}{dt} = \dot{m}_{H_2-in} - \left(\rho_{H_2}UA_r\right)_{out} - \frac{1}{2F} \tag{10}$$

$$\frac{V_a}{RT}\frac{dp_{O_2}}{dt} = \dot{m}_{O_2-in} - \left(\rho_{O_2}UA_r\right)_{out} - \frac{1}{4F} \tag{11}$$

The energy balance in the air-cooled fuel cell was expressed by equation (12).

$$\frac{dT}{dt} = 65i^2\frac{(R_a + R_{int})}{C_{ht}} - \frac{C_{ht}(T - T_r)}{R_t} \tag{12}$$

The rate of hydrogen production in the electrolyzer is given by Faraday's Law as shown in equation (13).

$$n_{H_2} = \frac{n_F n_C i_e}{2F} \tag{13}$$

Finally, the relationship between the theoretical and actual maximum amount of hydrogen produced by the electrolyzer is given by equation (14).

$$n_F = 96.5exp\left(\frac{0.09}{i_e} - \frac{75.5}{i^2{}_e}\right) \tag{14}$$

The dynamics of the power of the PEM fuel cell, which operates in cases of low electricity generation using wind and solar resources to meet the demand of 200W, is shown in Fig. 3 of the four locations studied.

3.3. A dynamic model of the photovoltaic solar panel.

The model used for the photovoltaic solar system is described by equations (15) - (19), with parameters and operational values available in modeling studies of hybrid systems. [32]–[34], where the panel current is given by equation (15) [28].

$$I_{ph} = [I_{SCr} + K_i(T - 298)] \times 0.001\lambda \tag{15}$$

In the same way, the inverse saturation current is defined. (I_{rs}) and the saturation current (I_o), which is dependent on the temperature of the panel, are given by the equations (16) y (17) respectively.

$$I_{rs} = \frac{I_{SCr}}{\left[exp\left(\frac{qVoc}{N_s kAT}\right) - 1\right]} \quad (16)$$

$$I_o = I_{rs}\left(^{T}/_{T_r}\right)^3 exp\left[\left(\frac{qE_{go}}{Bk}\right)\left(\frac{1}{T_r} - \frac{1}{T}\right)\right] \quad (17)$$

The output current of the cell corresponds to equation (18).

$$I_{PV} = N_p \times I_{ph} - N_p \times I_o\left[exp\left(\frac{q \times (V_{pv} + I_{PV}R_s)}{N_s AKT}\right) - 1\right] \quad (18)$$

where $V_{pv} = V_{OC,}N_p = 1\ y\ N_s = 36$. Finally, the total power is given by the equation (19).

$$P_{PV} = V_{PV} \times I_{PV} \quad (19)$$

The performance of the photovoltaic cell is related to the solar irradiation available at the site of operation of the system, which for this study was based on the year 2013. [35], resulting in the behavior shown in Fig. 4.

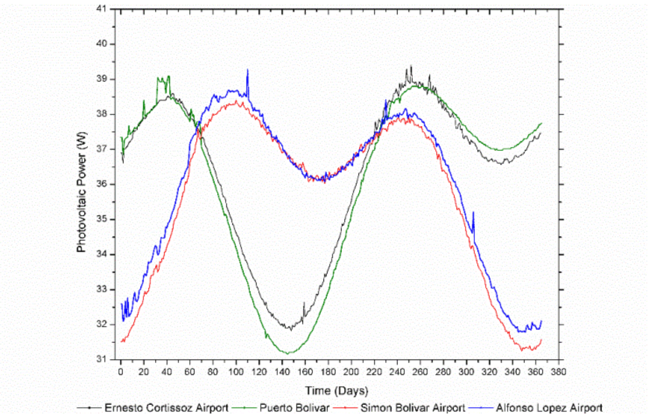

Fig. 4. Photovoltaic power response for Ernesto Cortissoz, Puerto Bolívar, Simón Bolívar and Alfonso López.

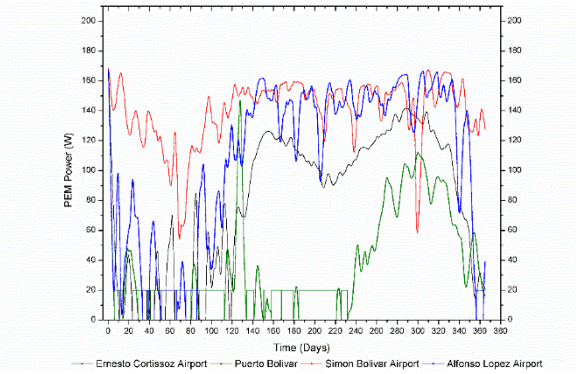

Fig. 3. PEM power response for Ernesto Cortissoz, Puerto Bolívar, Simón Bolívar and Alfonso López.

3.4. Dynamic model of the wind turbine.

The third source of energy presented in the hybrid system was wind energy, which is a function of wind speed at the operating height of the wind turbine. For the projection of wind speed at axle height, Hellmann's law was applied. [36] As shown in equation (20).

$$\frac{v}{v_o} = \left(\frac{h}{h_o}\right)^{\propto} \quad (20)$$

where v is the wind speed at height h to be calculated, v_o is the wind speed at a reference height h_o and $\propto$ is the wind velocity at the altitude of is the relative roughness, values available for these places in the wind Atlas [36].

The dynamic behavior of the power generated by the wind turbine operating in each of the study sites is shown in Fig. 5.

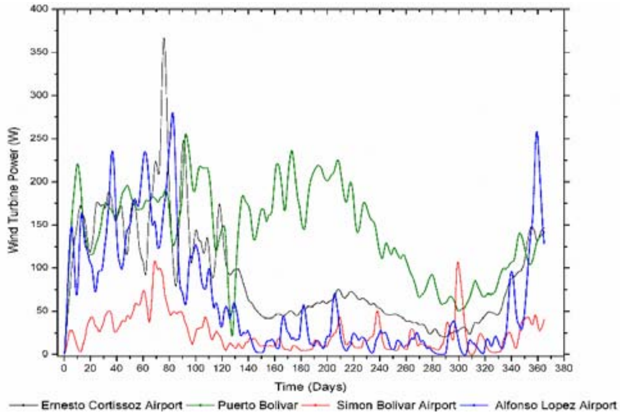

Fig. 5. Dynamic behavior of the wind power through a complete year at 100 meters high.

4. Results and analysis

Under the dynamic conditions established by the HEPGS in the different places of interest, the complementarity of solar and wind energy with the energy delivered by the PEM cell was evaluated to supply the 200W demand. To achieve the desired power in the cell, the molar flow of oxygen and hydrogen was regulated by PID controllers, obtaining the flow behavior shown in Fig. 6 and Fig. 7. For the case of Ernesto Cortissoz Airport as shown in Fig. 6, during January to August the cell operated at a low loading rate with the molar flow for hydrogen and oxygen of 7.50e-05 mol/s for both because wind power generation along with solar energy supplied 67.7% of the total energy generated. However, from September to December, the flows had a variation between 0.0005 to 0.0045 mol/s which meant a contribution of 53.45% cell equivalent to 427.61W. For the case of the Puerto Bolívar station, both the molar flow of hydrogen and oxygen that entered the PEM cell presented a constant behavior throughout the year with a value of 0.000075 mol/s as shown in the Fig. 6 due to the significant amount of wind energy generated, presenting a total of 2159.26W (81.168%) of total wind and solar power generation and for the cell a total of 484.32W (18.32%) for the whole year 2013. As to the behavior of the system operating at Simón Bolívar Airport, during the period from January to March. The cell, produced with a low molar flow regime of both hydrogen and oxygen with a value of 0.0075 mol/s, reaching the generation of wind and solar energy 40% of the total energy generated, while in early April to December, the PEM-type cell required the maximum molar flow of hydrogen and oxygen with a value of 0.0035 mol/s and 0.0017 mol/s respectively, generating a total of 1314.69 W (73.03%).

Finally, the operation of the system at Alfonso López Airport, led to the cell having a low charge generation between January and early August, with a value of 7.50e-05 mol/s for the input of hydrogen and oxygen flow, thus giving a combined production between solar and wind power of 58.41%, while for molar flow of oxygen presented the first change on Saturday August 3,2013 with a value of 0.0017 mol/s and hydrogen for Friday, August 9th with a value of 0.00119 mol/s as shown in Fig. 7, which was associated to the significant change in meteorological conditions, caused by a decrease in wind speed in the place so that the generation of the wind and solar component of the system decreased so that the PEM started to generate energy to supply the demand. In order, to provide the energy demand at critical operational points, the cell reached the molar flow values of hydrogen and maximum oxygen at the beginning of August and December, with values of 0.0035 mol/s and 0.0017 mol/s respectively, operational points that represented an energy generation of 1015.78 W (66.84%).

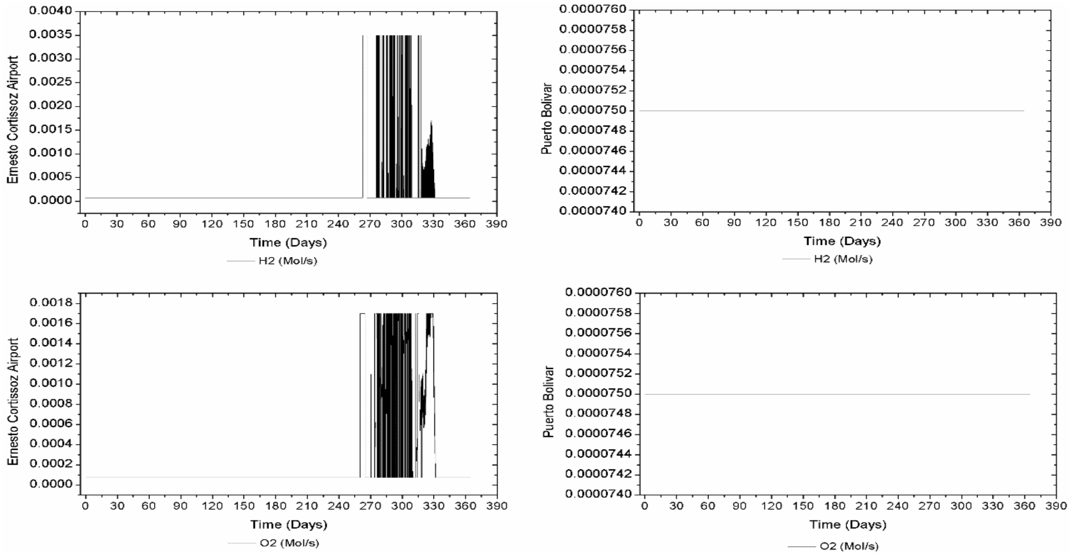

Fig. 6. Hydrogen and molecular oxygen at the entrance to Ernesto Cortissoz Airport and Puerto Bolívar Airport.

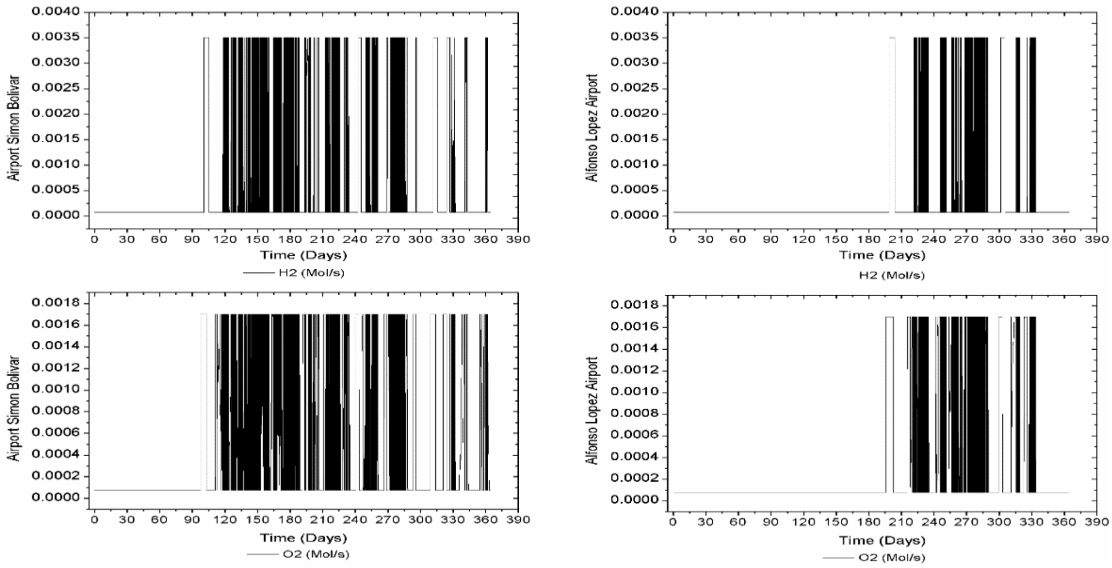

Fig. 7. Hydrogen and molecular oxygen at the entrance of the cell for Simón Bolívar and Alfonso López Airport.

The variations in the voltage and electrical current in the cell for the places studied are shown in Fig. 8, where it is highlighted that the maximum value of the current was presented for Alfonso López Airport with an amount of 3.97A at the end of May because at this time the speed of viewing was about 85% below its average value as shown in Fig. 5. On the other hand, the maximum voltage was not presented in the same place, but at Ernesto Cortissoz airport with a value of 61.8V for January 16, values that were the result of a cell power of 12.675W, which is a low contribution of this component (1.13%) compared to the other days of January, where the cell reached percentage peaks of generation on January 1 and 2 with values of 144.62W and 123.79W respectively.

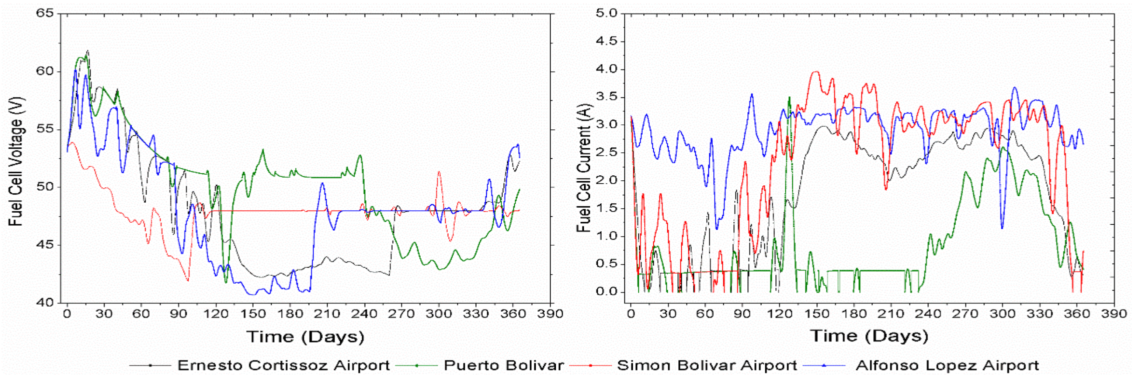

Fig. 8. Fuel cell electrical voltage and current at Ernesto Cortissoz, Puerto Bolivar, Simon Bolivar and Alfonso López.

For the demand of 200W, the respective values for each energy source were obtained, allowing the complementarity of these energy alternatives to be evaluated in each station, where similar behavior is highlighted for the power generated by the photovoltaic solar panel in all the study sites. Additionally, it was determined that the PEM-type cell produced more energy in September for the Simón Bolívar airport with a monthly power of 158,358W (9.45%), while the lower value was presented in Puerto Bolívar with 18,141W (3.745%) as shown in Fig. 9, in which in the same way it can be observed that in some months the demand is exceeded since the cell cannot stop operating and the compliment with wind and solar energy exceeds the demand, implying storage of this in a bank of capacitors.

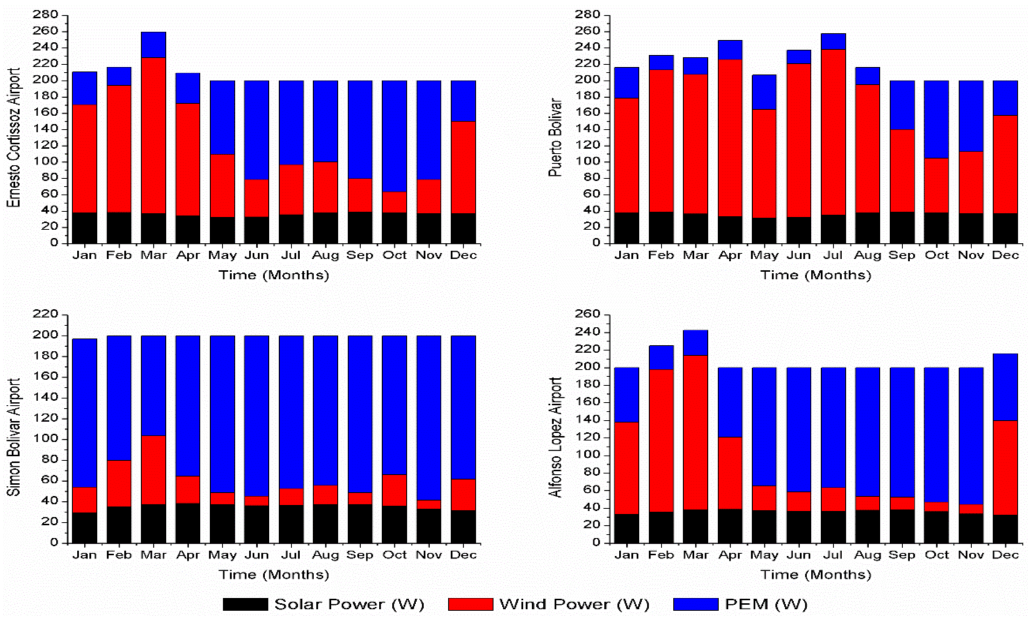

Fig. 9. Accumulated power from different energy sources for different sub-stations.

5. Conclusions

In the countries where hybrid power generation systems have been implemented and used, positive results in the energy transition have been achieved due to the advantages of renewable energy generation systems. In Colombia, specifically in the Caribbean region, there is a significant renewable resource that, when complemented with electrochemical generation systems such as the cell in a hybrid system, presents results of high operational viability. When evaluating the performance of the system in the different places studied, a similar solar power the profile noted due to the proximity of these places in the Colombian Caribbean region. As for the wind power generated, there is a significant difference between the Puerto Bolívar station and the others, which is why the implementation of a PEM is of great help in departments such as Magdalena, where the almost obligatory use of the PEM is indicated for the demand of 200W. However, for the case of the station located in Guajira (Puerto Bolívar), the use of PEM does not have a significant effect on the overall generation of the system, given that at this point the highest wind power values in the country are presented, implying a low load operation of the PEM type cell. The results on the wind energy generated show the stock of areas that can be estimated as essential wind resources, such as Puerto Bolívar and Ernesto Cortissoz airport, places where the hybrid system would operate with the low load cell.

References

[1] S. Ahmed, A. Mahmood, A. Hasan, G. A. S. Sidhu, and M. F. U. Butt, "A comparative review of China, India and Pakistan renewable energy sectors and sharing opportunities," *Renew. Sustain. Energy Rev.*, vol. 57, pp. 216–225, May 2016.

[2] A. Sinha, "Inequality of renewable energy generation across OECD countries: A note," *Renew. Sustain. Energy Rev.*, vol. 79, pp. 9–14, Nov. 2017.

[3] K. Kim, H. Park, and H. Kim, "Real options analysis for renewable energy investment decisions in developing countries," *Renew. Sustain. Energy Rev.*, vol. 75, pp. 918–926, Aug. 2017.

[4] A. K. Shukla, K. Sudhakar, and P. Baredar, "Renewable energy resources in South Asian countries: Challenges, policy, and recommendations," *Resour. Technol.*, vol. 3, no. 3, pp. 342–346, Sep. 2017.

[5] M. López-Losana, "Análisis de la producción científica sobre patología dual en prisión," p. 218, 2013.

[6] L. M. Romo Fernández, V. P. Guerrero Bote, and F. Moya Anegón, "Análisis de la producción científica española en energías renovables, sostenibilidad y medio ambiente (Scopus, 2003-2009) en el contexto mundial," *Investig. Bibl. Arch. Bibl. e Inf.*, vol. 27, no. 60, pp. 125–151, May 2013.

[7] L. M. Romo-Fernández, C. López-Pujalte, V. P. Guerrero Bote, and F. Moya-Anegón, "Analysis of Europe's scientific production on renewable energies," *Renew. Energy*, vol. 36, no. 9, pp. 2529–2537, Sep. 2011.

[8] A. Holma *et al.*, "Environmental impacts and risks of the national renewable energy targets – A review and a qualitative case study from Finland," *Renew. Sustain. Energy Rev.*, vol. 82, pp. 1433–1441, Feb. 2018.

[9] Congreso de Colombia, "Ley N° 1715 del 13 de mayo de 2014," *Upme*, no. May, p. 26, 2014.

[10] S. A. Abbasi, Tabassum-Abbasi, and T. Abbasi, "Impact of wind-energy generation on climate: A rising specter," *Renew. Sustain. Energy Rev.*, vol. 59, pp. 1591–1598, 2016.

[11] N. Kannan and D. Vakeesan, "Solar energy for the future world: - A review," *Renew. Sustain. Energy Rev.*, vol. 62, pp. 1092–1105, 2016.

[12] M. R. Islam, S. Mekhilef, and R. Saidur, "Progress and recent trends of wind energy technology," *Renew. Sustain. Energy Rev.*, vol. 21, pp. 456–468, 2013.

[13] Procolombia, "Electric Power in Colombia. Power Generation - 2015," p. 23, 2015.

[14] M. Y. Recalde, D. H. Bouille, and L. O. Girardin, "LIMITATION PARA EL DESARROLLO DE ENERGÍAS RENOVABLES EN ARGENTINA," *Probl. Desarro.*, vol. 46, no. 183, pp. 89–115, Oct. 2015.

[15] F. B. Budes, Y. C. Escorcia, and G. V. Ochoa, "Optimization of a Biomass , solar and fuel cell Hybrid energy systems for a specific energy load using Homer Pro software ®," vol. 11, no. 1, pp. 335–340, 2018.

[16] M. Sikka, T. F. Thornton, and R. Worl, "Sustainable Biomass Energy and Indigenous Cultural Models of Well-being in an Alaska Forest Ecosystem.," *Ecol. Soc.*, vol. 18, no. 3, pp. 531–543, 2013.

[17] A. Vides-Prado *et al.*, "Techno-economic feasibility analysis of photovoltaic systems in remote areas for indigenous communities in the Colombian Guajira," *Renew. Sustain. Energy Rev.*, vol. 82, pp. 4245–4255, Feb. 2018.

[18] "Sistema de Informacion Eléctrico Colombiano (SIEL)," 2018. [Online]. Available: http://www.siel.gov.co/Inicio/CoberturadelSistemaIntercontecadoNacional/ConsultasEstadisticas/tabid/81/Default.aspx. [Accessed: 22-Feb-2018].

[19] M. Mikati, M. Santos, and C. Armenta, "Modelado y Simulación de un Sistema Conjunto de Energía Solar y Eólica para Analizar su Dependencia de la Red Eléctrica," *Rev. Iberoam. Automática e Informática Ind. RIAI*, vol. 9, no. 3, pp. 267–281, Jul. 2012.

[20] C. Bordons, F. García-Torres, and L. Valverde, "Gestión Óptima de la Energía en Microrredes con Generación Renovable," *Rev. Iberoam. Automática e Informática Ind. RIAI*, vol. 12, no. 2, pp. 117–132, Apr. 2015.

[21] A. López, J. A. Somolinos, and L. R. Núñez, "Modelado Energético de Convertidores Primarios para el Aprovechamiento de las Energías Renovables Marinas," *Rev. Iberoam. Automática e Informática Ind. RIAI*, vol. 11, no. 2, pp. 224–235, Apr. 2014.

[22] C. L. de A. Dias, D. A. Castelo Branco, M. C. Arouca, and L. F. Loureiro Legey, "Performance estimation of photovoltaic technologies in Brazil," *Renew. Energy*, vol. 114, pp. 367–375, Dec. 2017.

[23] D. Abbes, A. Martinez, and G. Champenois, "Life cycle cost, embodied energy and loss of power supply probability for the optimal design of hybrid power systems," *Math. Comput. Simul.*, vol. 98, pp. 46–62, 2014.

[24] B. Parida, S. Iniyan, and R. Goic, "A review of solar photovoltaic technologies," *Renew. Sustain. Energy Rev.*, vol. 15, no. 3, pp. 1625–1636, 2011.

[25] G. Chicco and P. Mancarella, "A unified model for energy and environmental performance assessment of natural gas-fueled poly-generation systems," *Energy Convers. Manag.*, vol. 49, no. 8, pp. 2069–2077, 2008.

[26] Y. Cancino-Solórzano and J. Xiberta-Bernat, "Statistical analysis of wind power in the region of Veracruz (Mexico)," *Renew. Energy*, vol. 34, no. 6, pp. 1628–1634, Jun. 2009.

[27] O. del C. Colombiano, "Región Caribe Colombiana," 2015. [Online]. Available: http://www.ocaribe.org/region-caribe.

[28] N. Pandiarajan, R. Ramaprabha, and R. Muthu, "Application of circuit model for photovoltaic energy conversion system," *Int. J. Photoenergy*, vol. 2012, 2012.

[29] G. Valencia Ochoa, C. Blanco, C. Martinez, and E. Ramos, "Fuzzy Adaptive Control Applied to a Hybrid Electric-Power Generation System (HEPGS)," *Indian J. Sci. Technol.*, vol. 10, no. 41, pp. 1–9, 2017.

[30] S. Esmaeili and M. Shafiee, "Simulation of Dynamic Response of Small Wind-Photovoltaic-Fuel Cell Hybrid Energy System," vol. 2012, no. August, pp. 194–203, 2012.

[31] G. N. D. Sens S., "Anaerobic tratment of real textile wastewater with a fluidized bed reactor," *Water Res*, p. 37, 2003.

[32] J. Gabriel García Clúa, R. Julián Mantz, and H. De Battista, "Hybrid control of a photovoltaic-hydrogen energy system," *Int. J. Hydrogen Energy*, vol. 33, no. 13, pp. 3455–3459, Jul. 2008.

[33] Krismadinata, N. A. Rahim, H. W. Ping, and J. Selvaraj, "Photovoltaic Module Modeling using Simulink/Matlab," *Procedia Environ. Sci.*, vol. 17, pp. 537–546, Jan. 2013.

[34] J. J. Hwang, L. K. Lai, W. Wu, and W. R. Chang, "Dynamic modeling of a photovoltaic hydrogen fuel cell hybrid system," *Int. J. Hydrogen Energy*, vol. 34, no. 23, pp. 9531–9542, Dec. 2009.

[35] R. V. Padilla, G. Demirkaya, D. Y. Goswami, E. Stefanakos, and M. M. Rahman, "Heat transfer analysis of parabolic trough solar receiver," *Appl. Energy*, vol. 88, no. 12, pp. 5097–5110, 2011.

[36] G. Valencia Ochoa, M. Vanegas Chamorro, and J. Polo Jiménez, *Análisis estadístico de la velocidad y dirección del viento en la región caribe colombiana con énfasis en la Guajira*. 2016.